

# Confinement order parameters and fluctuations

Tina Katharina Herbst,<sup>1</sup> Jan Luecker,<sup>1,2</sup> and Jan M. Pawłowski<sup>1,3</sup>

<sup>1</sup>*Institut für Theoretische Physik, Universität Heidelberg,  
Philosophenweg 16, D-69120 Heidelberg, Germany*

<sup>2</sup>*Institut für Theoretische Physik, Goethe-Universität Frankfurt,  
Max-von-Laue-Straße 1, D-60438 Frankfurt/Main, Germany*

<sup>3</sup>*ExtreMe Matter Institute EMMI, GSI Helmholtzzentrum für  
Schwerionenforschung mbH, Planckstraße 1, D-64291 Darmstadt, Germany*

We study order parameters for the confinement-deconfinement phase transition related to the Polyakov-loop variable. The functional renormalisation group is used to compute these order parameters in a unified, non-perturbative continuum approach. Our result for the expectation value of the traced Polyakov loop agrees quantitatively with the lattice result. Furthermore, we discuss how this order parameter differs from the standard continuum Polyakov loop. For temperatures close to the phase transition temperature there are significant deviations. We argue that these deviations are of crucial importance for QCD effective models, which usually implicitly rely on a Gaussian approximation neglecting this difference.

PACS numbers: 12.38.Aw, 25.75.Nq, 05.10.Cc

## I. INTRODUCTION

The physics of low energy QCD is mainly governed by two phenomena: spontaneous chiral symmetry breaking and confinement. Order parameters for the former are local observables that are not invariant under chiral transformations, most prominently the chiral condensate. In turn, a smoking gun for confinement is the linear rise of the static quark-potential at infinite distance in pure  $SU(N)$  Yang-Mills theory. The underlying symmetry is the  $Z_N$ -center symmetry, which is only accessible via non-local observables such as the traced Polyakov loop. In QCD at the physical point, none of these symmetries is fully realised and the respective phase transitions turn into crossovers: chiral symmetry is explicitly violated by the current quark masses and the chiral anomaly, and center symmetry is violated explicitly by dynamical quarks in the fundamental representation. Nonetheless, the respective order parameters are interesting observables in full QCD as they give access to the amount of explicit symmetry breaking, and hence the proximity of QCD at finite temperature and density to a potential critical end-point in the phase diagram.

The confinement-deconfinement phase transition, or more precisely the transition from the quark into the hadronic phase, is also accessible with baryonic observables such as baryonic fluctuations. The latter are directly accessible within experiments and are hence especially interesting. In this context, observables based on the Polyakov-loop variable are of specific interest as the related gluonic backgrounds play an important rôle in the computation of the baryonic fluctuations, see [1].

More generally, in functional approaches to QCD the temporal gluonic background  $\langle A_0 \rangle$  relates to the Polyakov loop. It provides a natural expansion point for systematic expansions of first-principle QCD, as well as for QCD-enhanced low-energy effective models, see e.g. [2–7] and the recent survey [8]. This approach has

been established in [2, 9–12]. There it has been worked out how to define and compute the gauge invariant non-perturbative glue potential  $V[A_0]$  in Yang-Mills theory and QCD within the functional renormalisation group, as well as general functional methods. It has also been shown that the expectation value  $\langle A_0 \rangle$  of the gluonic background, defined as the minimum of the glue potential  $V[A_0]$ , serves as a gauge-invariant order parameter for the confinement-deconfinement phase transition. It is indeed directly linked to the gauge-invariant eigenvalues of the untraced Polyakov loop. Moreover, the setting enabled us to link the confinement-deconfinement phase transition algebraically to a mass gap in the gluon propagator, [9, 12]. In the latter work [12], the framework has been extended to general functional approaches including the Dyson-Schwinger equations and the 2PI formalism, for applications to QCD see [13–15]. In [16–18] the approach has been extended to the Coulomb gauge in the Hamiltonian formulation. It has also been picked up in more phenomenological applications to QCD, see e.g. [19–23].

In the present work we study the relation between the expectation value of the traced Polyakov loop and the expectation value  $\langle A_0 \rangle$ , the temporal gluonic background of the theory, including the gauge invariant definition of the latter. In Secs. II and III of this work we show how these order parameters for the confinement-deconfinement phase transition are derived from the Polyakov loop, and discuss their properties and the underlying symmetries. Subsequently we set up the functional renormalisation group (FRG) as a framework to study these objects in a unified approach, see Sec. IV. Notably, we present the first non-perturbative continuum calculation of the expectation value of the traced Polyakov loop, which is a standard observable on the lattice. We discuss the renormalisation of this object in Sec. V and demonstrate the quantitative agreement with the lattice results in Sec. VI.

## II. ORDER PARAMETERS AND THE POLYAKOV LOOP

In the present work we compute and compare different order parameters for the confinement-deconfinement phase transition that can be derived from the Polyakov loop. The properties of the Polyakov loop itself and related constructions of order parameters have been discussed at length in the literature. This includes the discussion of simple representations in physical gauges such as the Polyakov gauge, maximal Abelian gauges and axial gauges. The latter gauges, and in particular the Polyakov gauge, also facilitate the access to topological excitations or defects and their rôle for the confinement-deconfinement phase transition, see e.g. [24, 25] and references therein. Here we briefly review some important properties.

The Polyakov loop, the Wilson loop in the temporal direction, is defined as

$$P(\vec{x}) = \mathcal{P} \exp \left\{ ig \int_0^\beta dx_0 A_0(x_0, \vec{x}) \right\}, \quad \text{with} \quad \beta = \frac{1}{T}, \quad (1)$$

where  $\mathcal{P}$  denotes path ordering, and  $g$  the gauge coupling. Due to the periodicity in the temporal direction,  $x_0 \rightarrow x_0 + \beta$ , gauge fields have to be periodic up to gauge transformations, the temporal transition functions  $t_0(x)$ . The latter can be chosen periodic,  $t_0(x_0 + \beta, \vec{x}) = t_0(x_0, \vec{x})$ . Under general gauge transformations  $U(x_0, \vec{x})$ , the Polyakov loop transforms as

$$P(\vec{x}) \rightarrow U^{-1}(0, \vec{x}) P(\vec{x}) U(\beta, \vec{x}). \quad (2)$$

Notably, the traced Polyakov loop,  $\text{Tr} P(\vec{x})$ , is only invariant under periodic gauge transformations with  $U(x_0 + \beta, \vec{x}) = U(x_0, \vec{x})$ , that also guarantee the periodicity of the transition function  $t_0$ . Under these periodic gauge transformations (1) transforms as a tensor

$$P(\vec{x}) \rightarrow U^{-1}(\vec{x}) P(\vec{x}) U(\vec{x}), \quad \text{with} \quad U(\vec{x}) = U(0, \vec{x}), \quad (3)$$

and the traced Polyakov loop is invariant. In turn, under non-periodic gauge transformations the periodicity of the temporal transition functions changes and  $P(\vec{x})$  has to be augmented by transition functions in order to provide a tensor under gauge transformations. This generalisation is necessary e.g. if a temporal axial gauge is considered with  $A_0 = 0$ . Clearly  $P(\vec{x}) = \mathbb{1}$  in such a gauge and carries no physics information. Then, the information about the phase transition is comprised entirely in the transition functions, see e.g. [24] for more details.

Here, however, we resort to the periodic setting. Then one well-known standard order parameter is given by the expectation value of the trace of the Polyakov loop. The normalised trace reads

$$L[A_0] = \frac{1}{N} \text{Tr}_f P(\vec{x}), \quad (4)$$

which is gauge invariant under periodic gauge transformations. The expectation value of (4),  $\langle L[A_0] \rangle$ , relates

to the free energy,  $F_{q\bar{q}}$ , of a static quark–anti-quark pair at infinite distance,

$$\langle L[A_0] \rangle \sim e^{-\frac{1}{2}\beta F_{q\bar{q}}}. \quad (5)$$

Since the free energy of a quark–anti-quark pair is finite in the deconfined phase and diverges in the confined phase, one can deduce that  $\langle L[A_0] \rangle$  indeed is an order parameter for the confinement-deconfinement transition. More precisely, it is an order parameter for center symmetry breaking: transformations with  $z \in Z_N$  transform the Polyakov loop into

$$P(\vec{x}) \rightarrow zP(\vec{x}) \quad \Rightarrow \quad L[A_0] \rightarrow zL[A_0], \quad (6)$$

where  $z$  in (6) is in the fundamental representation. Hence, in the center-symmetric phase the expectation value of  $L$  has to vanish. In turn, the ground state in the perturbative high-temperature phase is given by vanishing gauge fields which break center symmetry maximally. Then we have  $\langle L[A_0] \rangle > 0$ , if we single out the group direction that gives real and positive values for the Polyakov loop. This can either be done by a small explicit symmetry breaking in the effective Polyakov loop potential or by appropriate temporal boundary conditions, both are common procedures for computing the order parameters of spontaneous symmetry breaking. We are finally led to

$$\langle L[A_0] \rangle \begin{cases} = 0 & \text{for } T < T_c \\ > 0 & \text{for } T > T_c \end{cases}. \quad (7)$$

As the underlying symmetry is the discrete  $Z_N$ -symmetry, we expect a second-order phase transition for  $SU(2)$  and a first-order transition for  $SU(N > 2)$ . This has indeed been verified on the lattice as well as in the continuum. Moreover, the temperature-dependence of the order parameter shows rapid convergences towards the large- $N$  limit, for results in the present continuum QCD setting and on the lattice see e.g. [11, 26]. Despite this successful classification of the confinement-deconfinement phase transition in semi-simple Lie groups there are strong indications that it is the number of degrees of freedom that triggers the order of the confinement-deconfinement phase transition, rather than the center. For example, for exceptional Lie groups one sees first-order phase transitions, e.g. [11], while for  $SO(3)$  a second order phase transition is observed, e.g. [27].

The expectation value of the traced Polyakov loop (7) is a simple order parameter for the confinement-deconfinement phase transition which is easily accessible on the lattice. In terms of the gauge field, however, it requires the computation of infinite-order correlation functions of the temporal gauge field. Hence, within continuum computations based on a description in gauge fields this asks for the definition of an order parameter which is more easily accessible. To this end we note that the

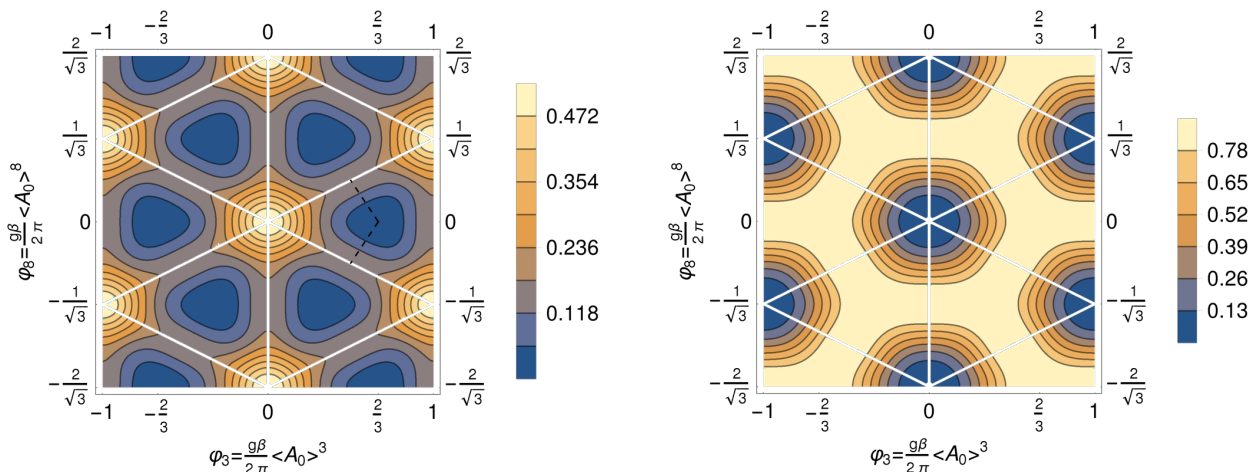


FIG. 1. Equipotential lines of the glue potential,  $V(\varphi_3, \varphi_8)$ , in the confined phase (left,  $T = 236$  MeV) and in the deconfined phase (right,  $T = 384$  MeV). Lighter colours indicate higher potential values. The periodicity of the potential is clearly visible. The triangles are the Weyl chambers and Weyl reflections are the reflections about the edges of the Weyl chambers. The centers of the Weyl chambers single out the center symmetric points of the Polyakov loop.

Polyakov loop (1) can also be written as the exponential of an algebra-valued field  $\varphi$ ,

$$P(\vec{x}) = e^{2\pi i \varphi(\vec{x})}, \quad \text{with} \quad \varphi(\vec{x}) \rightarrow U^{-1}(\vec{x}) \varphi(\vec{x}) U(\vec{x}). \quad (8)$$

The transformation property of  $\varphi$  in (8) follows straightforwardly from that of the Polyakov loop (3). Hence,  $\varphi$  also transforms as a tensor under gauge transformations. This entails that the eigenvalues  $\nu_n$  of  $\varphi$  are gauge invariant, as gauge transformations are unitary rotations that do not change the eigenvalues of a matrix. We utilise this freedom and rotate  $\varphi$  into the Cartan subalgebra. We shall briefly discuss below that this amounts to taking the Polyakov gauge. Then, the gauge-invariant eigenvalues are given by the relation

$$\varphi(\vec{x})|\phi_n\rangle = \nu_n(\vec{x})|\phi_n\rangle, \quad (9)$$

with eigenvectors  $|\phi_n\rangle$  that span the Cartan subalgebra. This allows us to define a constant background

$$\bar{\varphi} = \sum_n \langle \nu_n | \phi_n \rangle \langle \phi_n |, \quad (10)$$

which carries the gauge invariant information about the eigenvalues of the Polyakov loop,  $\exp\{2\pi i \nu_n\}$ , and hence about the confinement-deconfinement phase transition. Note that for the expectation values  $\langle \nu_n \rangle$  a preferred group direction has to be singled out, similarly to the computation of the expectation value of the traced Polyakov loop.

Indeed,  $\bar{\varphi}$  itself is an order parameter, which can be deduced from the transformation properties of  $\varphi$  under center transformations. Before this is detailed, let us remark that in the Polyakov gauge there is a simple relation between the algebra-valued field  $\varphi$  and the gauge field. The Polyakov gauge reads

$$A_0(x) = A_0^c(\vec{x}), \quad (11)$$

where  $A_0$  depends on the spatial coordinates  $\vec{x}$  only and is rotated into the Cartan subalgebra indicated by the superscript  $c$  in (11). Then we have

$$2\pi\varphi(\vec{x}) = g\beta A_0^c(\vec{x}). \quad (12)$$

The relation (12) entails that the eigenvalues of  $g\beta A_0^c(\vec{x})$  in Polyakov gauge are the gauge-invariant eigenvalues of  $\varphi$ . Hence, despite working in a gauge-fixed setting, we can directly extract gauge-invariant information from the expectation value of the gauge field. With (12) the traced Polyakov loop (4) then takes the simple form

$$L[A_0] = \frac{1}{N} \text{Tr}_f e^{ig\beta A_0^c} = \frac{1}{N} \text{Tr}_f e^{2\pi i \varphi} =: L(\varphi). \quad (13)$$

Note also that (12) holds for any constant gauge field as constant fields can be rotated in the Cartan subalgebra. For these fields in  $SU(2)$  we have  $\beta g A_0 = 2\pi\varphi_3 \sigma^3/2$  with the generator  $\sigma^3/2$  of the Cartan subalgebra. For  $SU(3)$  we write

$$\beta g A_0 = 2\pi (\varphi_3 t^3 + \varphi_8 t^8) =: 2\pi\varphi, \quad (14)$$

with  $t^3, t^8$  the generators of the Cartan subalgebra of  $SU(3)$ . With (14) the traced Polyakov loop in  $SU(3)$  Yang-Mills theory takes the form

$$L(\varphi_3, \varphi_8) = \frac{1}{3} \left( e^{-\frac{2\pi i \varphi_8}{\sqrt{3}}} + 2 \cos(\pi \varphi_3) e^{\frac{\pi i \varphi_8}{\sqrt{3}}} \right). \quad (15)$$

The above entails that the corresponding effective potential  $V(\varphi)$  simply is that of constant temporal gauge fields  $V[A_0]$ . The expectation value  $\bar{\varphi}$  can be determined from the minimum of the effective potential  $V(\varphi)$ . As for  $\langle L[A_0] \rangle$ , we single out the minimum with  $L(\bar{\varphi}) \in \mathbb{R}$  and positive, leading to  $\varphi_8 = 0$ , see (15). Contour plots of the effective potential both in the deconfined and in the confined phase are shown in Fig. 1, and details about its

continuum definition are provided in the next section. In the confined phase we have  $\bar{\varphi}_3 = 2/3$  and  $L[\bar{\varphi}] = 0$  while in the deconfined phase we have  $0 \leq \bar{\varphi}_3 < 2/3$ ,  $L[\bar{\varphi}] \neq 0$ , with  $\bar{\varphi}_8 = 0$  in both cases. This already indicates that  $\bar{\varphi}$  as well as  $L[\bar{\varphi}]$  are order parameters for center symmetry breaking.

Now we turn to the properties of  $\varphi$  and the expectation value  $\bar{\varphi}$  under symmetry transformations, and in particular center transformations. On the level of the algebra field  $\varphi$ , center symmetry is realised as a shift

$$\varphi \rightarrow \varphi + \theta_z, \quad \text{with} \quad z = e^{2\pi i \theta_z}. \quad (16)$$

The center transformation is a symmetry transformation of the effective potential  $V(\varphi)$ , as can be seen from the contour plots in Fig. 1. For  $SU(2)$  the center elements are given by  $z = \mathbb{1}, -\mathbb{1}$ . The corresponding algebra elements of  $z$  are  $\theta_z = 0, \sigma^3/2$  respectively, with the Pauli matrix  $\sigma_3$ . For  $SU(3)$  the center elements  $z$  and the corresponding algebra elements  $\theta_z$  are given by

$$z = \mathbb{1}, \mathbb{1}e^{\frac{2\pi}{3}i}, \mathbb{1}e^{\frac{4\pi}{3}i}, \quad \theta_z = 0, \frac{2}{\sqrt{3}}t^8, t^3 - \frac{1}{\sqrt{3}}t^8, \quad (17)$$

respectively with the Cartan generators  $t^3, t^8$  of  $SU(3)$  being half of the Gell-Mann matrices  $\lambda^3, \lambda^8$ .

The transformation (16) can be combined with a Weyl reflection, i.e. a reflection about the edges of the Weyl chamber. Weyl reflections are an isometry of the roots of the gauge group and are generated by specific constant gauge transformations. Hence they are a symmetry of the theory. In  $SU(2)$  they are simply given by  $\varphi \rightarrow -\varphi$ , while in  $SU(3)$  the Weyl reflections can be read off from Fig. 1. Clearly this is a symmetry of the potential. Restricting ourselves to the fundamental chamber, they map the chamber onto itself, and the centers of the Weyl chambers are fixed-points of the combined symmetry transformations, see e.g. [25] for a more detailed discussion. Hence, in the center-symmetric phase  $\bar{\varphi}$  has to settle at these points. We conclude that  $\bar{\varphi}$  and the Polyakov loop  $L[\bar{\varphi}]$  are indeed order parameters for the confinement-deconfinement phase transition,

$$L[\bar{\varphi}] \begin{cases} = 0 & \text{for } T < T_c \\ > 0 & \text{for } T > T_c \end{cases}, \quad (18)$$

where we have singled out the positive semi-definite minimum on the real axis, i.e.  $\bar{\varphi}^8 = 0$ .

### III. ORDER PARAMETERS AND GAUGE FIELDS

In the following we compute the order parameters, (7) and (18), within a non-perturbative approach to continuum Yang-Mills theory formulated in terms of the gauge fields  $A_\mu$ . Both order parameters can be expressed in terms of the temporal gauge field  $A_0$  and expectation values of correlations of  $A_0$ . We have already discussed

that the computation of  $\langle L[A_0] \rangle$  within an expansion in the gauge field requires the computation of infinite-order correlation functions of the gauge field. On the lattice, on the other hand, it is straightforward to compute  $\langle L[A_0] \rangle$ , see e.g. [28–34]. In this manner, the first-order nature of the phase transition in  $SU(3)$  with critical temperature  $T_c/\sqrt{\sigma} = 0.646$  in units of the string tension  $\sigma$  has been established. We shall see in Sec. IV B that within the functional renormalisation group the task of computing  $\langle L[A_0] \rangle$  in the continuum is also tractable. It can be reduced to solving a differential equation that is linear in the scale-derivative of  $L$  and its second  $\varphi$ -derivatives.

In turn, the computation of the order parameter (18) only requires the computation of the non-perturbative expectation value of the constant temporal background gauge field in a background-field approach, cf. [9, 12], or in the Polyakov gauge [10],

$$L[\langle A_0 \rangle] = \frac{1}{N} \text{Tr}_f e^{ig\beta \langle A_0 \rangle}. \quad (19)$$

The expectation value  $\langle A_0 \rangle$  is determined as the minimum of the non-perturbative effective glue background potential  $V[\bar{A}_0]$  in the background-field approach, e.g. [35]. To this end we introduce a background field  $\bar{A}_\mu$  by splitting the full gauge field linearly into

$$A_\mu = \bar{A}_\mu + a_\mu, \quad (20)$$

with  $\langle a_\mu \rangle = 0$ . The background field enters the background gauge-fixing condition

$$\bar{D}_\mu a_\mu = 0, \quad \text{with} \quad \bar{D}_\mu = \partial_\mu + ig\bar{A}_\mu. \quad (21)$$

The background-field effective action  $\Gamma_k[\bar{A}, \phi]$  depends on the background field  $\bar{A}_\mu$  and the fluctuation field  $\phi = (a_\mu, c, \bar{c}, \dots)$ . This setting allows for the definition of a gauge invariant effective action

$$\Gamma_k[A_\mu] = \Gamma_k[A_\mu, 0], \quad (22)$$

that is invariant under the gauge transformation

$$A_\mu \rightarrow -\frac{i}{g}(UD_\mu U^{-1}), \quad \text{with} \quad D_\mu = \partial_\mu + igA_\mu. \quad (23)$$

For constant fields this reduces to  $A_\mu \rightarrow UA_\mu U^{-1}$  as for  $\varphi$  in (8). The related effective background potential is given by

$$V[A_0] = \frac{1}{\beta\mathcal{V}} \Gamma[A_0], \quad (24)$$

where  $\mathcal{V}$  the spatial volume. It is evident from the discussion in the last section that Eq. (24) simply is the potential for constant  $\varphi$  with  $V(\varphi) = V[A_0(\varphi)]$  with the relation (14) for  $SU(3)$ .

In perturbation theory the effective potential  $V[A_0]$  (24) has first been computed in [36, 37]. It features only the deconfining minimum at  $A_0 = 0$ . A non-perturbative

approach for the computation of  $V[A_0]$  has been established in [9, 10, 12]. By now computations of the glue potential from a variety of methods have been put forward, including the FRG and Dyson-Schwinger equations, 2PI-schemes, perturbative approaches and the lattice [2, 9–13, 16–18, 20–22, 38–40].

The expectation value  $\bar{\varphi} = g\beta\langle A_0 \rangle / (2\pi)$  is then given by the minimum of the background effective potential, i.e. it is defined via

$$\left. \frac{\partial V[A_0]}{\partial A_0} \right|_{A_0=\langle A_0 \rangle} = 0, \quad \text{with } L[\langle A_0 \rangle] \geq 0. \quad (25)$$

As can be seen from Fig. 1, the minimum is not unique, and we choose the one which gives a real, positive semi-definite traced Polyakov loop via Eq. (13), cf. our discussion in Sec. II. The resulting critical temperature for  $SU(3)$  is in quantitative agreement with the lattice result with a critical temperature  $T_c/\sqrt{\sigma} = 0.655$  in units of the string tension  $\sigma$ , see [12]. Here, the biggest systematic uncertainty concerns the relative scale setting in the continuum and on the lattice, leading to a systematic error estimate of about 10% [12].

Note that the two order parameters derived from the Polyakov loop,  $\langle L[A_0] \rangle$  and  $L[\langle A_0 \rangle]$ , are indeed closely related: Jensen's inequality yields the relation [9]

$$\langle L[A_0] \rangle \leq L[\langle A_0 \rangle], \quad (26)$$

in the region where  $L[A_0]$  is convex. Furthermore we have, cf. [10, 12],

$$L[\langle A_0 \rangle] = 0 \Leftrightarrow \langle L[A_0] \rangle = 0. \quad (27)$$

Both these observables have been studied extensively and naturally reproduce the order of the phase transition as well as the critical temperature. However, the computations also reveal that the inequality (26) is far from being saturated. This statement holds for  $T > T_c$ , i.e. in the center broken phase in pure Yang-Mills theory, and for all temperatures in QCD.

For QCD effective models, e.g. [4, 5, 41–52] this is particularly important. There, one usually relies on input from other methods to fix the gauge sector. The common procedure is to introduce a Polyakov-loop potential  $V_L(L, \bar{L})$ , with  $\bar{L}$  being the conjugate Polyakov loop. The coefficients of  $V_L$  are then fitted to lattice Yang-Mills data, i.e. the potential is based on  $\langle L \rangle$ .

This has to be contrasted with the fact that most low-energy effective models can be derived from continuum QCD in a standard formulation with gauge fields. Hence, they should be formulated in terms of  $\langle A_\mu \rangle$ . Then, also the ultraviolet parameters of these models at their initial scale,  $\Lambda \approx 1$  GeV, can be determined from continuum QCD at this scale, and the gauge sector is related to the glue potential,  $V[A_0]$ .

Alternatively, a formulation in terms of  $\langle L \rangle$  is possible. Then, however, the matter part of the models is subject

to an inherent Gaussian approximation

$$\langle L_1 \cdots L_n \bar{L}_1 \cdots \bar{L}_m \rangle = \prod_{i=1}^n \langle L_i \rangle \prod_{j=1}^m \langle \bar{L}_j \rangle, \quad (28)$$

with the shorthand notation  $L_i = L(\vec{x}_i)$  and similarly for  $\bar{L}_j$ . Further reductions such as

$$\frac{1}{N^2} \langle \text{Tr } P_1 P_2 \rangle = \langle L_1 \rangle \langle L_2 \rangle, \quad (29)$$

with  $P_i = P(\vec{x}_i)$  are used. Eq. (29) neglects spatial fluctuations of the Polyakov-loop variable  $P(\vec{x})$ . Note that in the Gaussian approximation underlying (28) and (29), the inequality (26) saturates, which is most easily seen in the Polyakov gauge Eq. (11). In other words, the difference between the observables  $\langle L \rangle$  and  $L[\langle A_0 \rangle]$  encodes the non-Gaussianity of the Polyakov loop, and the explicit results show the failure of the Gaussian approximation. Thus, to achieve a consistent treatment of the gauge sector in QCD effective models, a reliable resolution of the deviation between these two quantities is of utmost importance. In the present work we fill this gap and compute both definitions of the Polyakov loop in a unified approach from the FRG.

Apart from its relevance for effective models, the calculation of  $\langle L \rangle$  from the FRG represents one more observable that is available both, in the continuum and on the lattice, and allows us to demonstrate that the relevant dynamics of the system is properly accounted for in the functional continuum approach.

#### IV. CONTINUUM APPROACH TO CONFINEMENT ORDER PARAMETERS

As already emphasised, the Polyakov loop  $\langle L[A_0] \rangle$  is a non-local and all-order correlation function of the temporal gauge field. First-principle continuum approaches to QCD, however, are based on the computation of local correlation functions of the fundamental fields, and in particular  $A_0$ . It is this difference that makes the continuum computation of  $\langle L[A_0] \rangle$  so difficult. At large momentum scales  $k \gg \Lambda_{\text{QCD}}$ , this problem is resolved within the perturbative expansion that allows us to drop the higher-order correlation functions due to the small gauge coupling. An extension of such a study into the non-perturbative domain is made feasible by functional methods. In the present work we resort to the functional renormalisation group (FRG).

##### A. Functional renormalisation group

The FRG allows us to systematically compute the scale dependence of correlation functions. To this end, an infrared regulator function,  $R_k$ , is introduced into the propagators of the theory. Such a regulator suppresses the



FIG. 2. Diagrammatic representation of the FRG flow for YM theory. Curly lines denote gluonic degrees of freedom, while dashed lines represent the ghost and anti-ghost. The black dot indicates the full propagator and the crossed circle symbolises the regulator insertion.

propagation of quantum and thermal fluctuations below the infrared cutoff scale  $k$ . Lowering the cutoff scale  $k$  implements the Wilsonian idea of integrating out fluctuations momentum shell by momentum shell. In the presence of the scale  $k$  the scale-dependent effective action,  $\Gamma_k$ , only carries the quantum and thermal physics of momentum fluctuations above the cutoff scale. In turn, all quantum and thermal fluctuations below this scale are suppressed. Hence  $\Gamma_k$  interpolates between the bare action at an ultraviolet scale  $\Lambda$ , and the full quantum effective action for  $k = 0$ . Its evolution is described by the Wetterich equation [53],

$$\partial_t \Gamma_k[\phi] = \frac{1}{2} \text{Tr} G_k[\phi] \dot{R}_k, \quad \text{with} \quad G_k[\phi] = \frac{1}{\Gamma_k^{(2)}[\phi] + R_k}, \quad (30)$$

and the trace sums over momenta, internal indices and species of fields, including minus signs for fermionic loops. In (30),  $\dot{R}_k = \partial_t R_k = k \partial_k R_k$  denotes the scale derivative of the regulator w.r.t. the FRG time,  $t = \log(k/\Lambda)$ , and  $G_k$  is the full propagator at the scale  $k$ . A pictorial representation of this equation is given in Fig. 2 for the special case of Yang-Mills (YM) theory used in this work. The curly line denotes the scale-dependent gluon propagators, while the dashed line represents the ghost propagator. The crossed circle symbolises the regulator insertion,  $\dot{R}_k$ . By virtue of the regulator function, (30) is ultraviolet and infrared finite. It has a one-loop structure, but is fully non-perturbative. The solution of this equation relies on the propagators, which themselves obey flow equations derived from (30), see [12, 54].

As can be seen from relation (24), the flow of the glue potential,  $V_k[A_0]$ , is directly related to that of the effective action,

$$\partial_t V_k[A_0] = \frac{1}{\beta \mathcal{V}} \partial_t \Gamma_k[A_0]. \quad (31)$$

Furthermore, in [55] a flow equation for general observables  $I_k = \langle \hat{I}_k[J, \hat{\phi}] \rangle$  has been derived, where  $\hat{\phi}$  is the quantum field with  $\phi = \langle \hat{\phi} \rangle$ . The flow equation for  $I_k$  reads

$$\partial_t I_k[\phi] = -\frac{1}{2} \text{Tr} \left\{ \left( G_k \dot{R}_k G_k \right)_{\mathbf{ab}} \frac{\delta}{\delta \phi_{\mathbf{b}}} \frac{\delta}{\delta \phi_{\mathbf{a}}} I_k[\phi] \right\}. \quad (32)$$

The bold letter indices  $\mathbf{a}, \mathbf{b}$  collect species of fields, Lorentz and internal indices and again,  $G_k$  denotes the

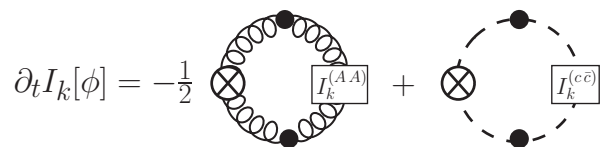


FIG. 3. Diagrammatic representation of the FRG flow (32) for general operators  $I_k[\phi]$  in YM theory. The boxes indicate the second functional derivative of the operator w.r.t. the gluon and ghost fields, respectively.

full propagator at RG-scale  $k$ . We refer the reader to [55] for more details and the derivation of (32), and to [55–63] for QCD-related reviews of the FRG.

Fig. 3 shows the diagrammatic representation of the flow (32), again for YM theory. Its structure is similar to Fig. 2, except for the presence of second derivatives of the operator  $I_k$  w.r.t. the fields, indicated by the boxes. Once more the propagators of the theory serve as input for the solution of this flow equation.

The set of operators  $I_k$  for which (32) is valid, includes, e.g., the (connected and disconnected)  $n$ -point correlation functions  $\{ \langle \phi_1 \phi_2 \dots \phi_n \rangle \mid n \in \mathbb{N} \}$  as well as  $\frac{\delta \Gamma}{\delta \phi}$ , cf. [55]. In particular, the observable  $I_k = \langle L[A_0] \rangle$  falls into this class of operators.

## B. Flow equation for the Polyakov loop

From now on we restrict our discussion to  $SU(3)$  Yang-Mills theory, full QCD will be discussed elsewhere. We use the covariant background-field formalism [35] with the background gauge-fixing condition (21) in the Landau-deWitt gauge. The vertices  $\Gamma^{(n)}$  of the effective action  $\Gamma_k[A_\mu]$  are directly related to S-matrix elements, and hence (22) directly carries physics information. Its flow equation is simply that of  $\Gamma_k[A_\mu, 0]$  in (30),

$$\partial_t \Gamma_k[A_0] = \frac{1}{2} \text{Tr} G_k[A_0] \dot{R}_k, \quad (33)$$

with

$$G_k[A_0] = \frac{1}{\frac{\delta^2 \Gamma_k}{\delta \phi^2} + R_k} [A_0, \phi = 0]. \quad (34)$$

Eqs. (33) and (34) entail that the propagators of the fluctuation fields evaluated at vanishing fluctuation field,  $G_k[A_0]$ , govern the flow of the gauge-invariant effective action. This is the peculiar situation that the flow of a gauge invariant quantity is governed by a gauge variant quantity, the fluctuation field propagator. The latter satisfies a complicated Slavnov-Taylor identity, see e.g. [55]. However, for vanishing fluctuation field,  $\phi = 0$ , the propagator, (34), is gauge covariant and can be expanded in gauge covariant tensors. It is this property that enables us to use the results of the Landau gauge, corresponding to the background Landau-deWitt gauge

(21), [9, 11, 12, 54]. The gauge covariance allows us to expand the two point correlator of the fluctuation field,  $\delta^2/\delta\phi^2\Gamma[A_0, 0](p^2)$  in Landau-deWitt gauge about the Landau gauge propagator [9, 12],

$$\frac{\delta^2\Gamma[A_0, 0]}{\delta\phi^2}(p) = \frac{\delta^2\Gamma_{\text{Lan}}}{\delta\phi^2}(D) + f(D, F, A_0), \quad (35)$$

where the covariant tensor  $f$  satisfies  $f(D, 0, 0) \equiv 0$  and the  $A_0$ -dependence of  $f(D, F, A_0)$  indicates the dependence on the covariant tensor  $P(\vec{x})$ . The subscript 'Lan' indicates the standard Landau gauge with  $\partial_\mu A_\mu = 0$ . The extension to covariant momenta is done such that  $D \cdot \delta^2/\delta A_0^2 \Gamma_{\text{Lan}}(D) = 0$ , up to the gauge fixing term. For constant fields the field-strength tensor vanishes,  $F = 0$ , and the covariant tensor reduces to  $f(D, A_0)$ .

Eq. (35) allows us to use the results of the finite temperature ghost and gluon propagators of [54] for the first term on the right-hand side of (35). The computation of  $f(D, F, A_0)$  will be discussed in Sec. IV C. The Landau gauge two point functions at finite temperature are conveniently parametrised as

$$\Gamma_{L/T,k}^{(2)}(p) = Z_{L/T,k}(p) p^2 P^{L/T}, \quad \Gamma_{\bar{c}c,k}^{(2)}(p) = Z_{c,k}(p) p^2, \quad (36)$$

where  $P^L$  and  $P^T$  are the projection operators onto the chromo-electric and chromo-magnetic gluon modes, and the identity matrix in colour space is implied. For more details see [54]. The following computation of Polyakov loop expectation values only implicitly depends on  $Z_T$ , which relates to the spatial components of the gauge field. For the sake of simplicity we hence denote

$$Z_{a,k}(p) = Z_{L,k}(p), \quad Z_{\bar{A},k}(p) = (Z_{\bar{A}})_{L,k}(p). \quad (37)$$

Both, the fluctuating,  $a_0$ , and the background,  $\bar{A}_0$ , wave-function renormalisations are the chromo-electric ones.

With this choice of gauge, the background temporal gauge field,  $\bar{A}_0$ , is in the Polyakov gauge. For vanishing fluctuation field,  $a_\mu = 0$ , we define, cf. Eqs. (10) and (14),

$$\beta \bar{g}_k Z_{\bar{A},k}^{1/2} \bar{A}_0 = 2\pi (\bar{\varphi}_3 t^3 + \bar{\varphi}_8 t^8) =: 2\pi \bar{\varphi}, \quad (38)$$

where we have made the wave-function renormalisation  $Z_{\bar{A},k} = Z_{\bar{A},k}(p_0 = 0, \vec{p}^2 = k^2)$  of the background field explicit. The wave-function renormalisation is evaluated at  $\vec{p}^2 = k^2$ , which is the important momentum scale in the flow. The running coupling  $\bar{g}_k$  is the background running coupling, evaluated at the symmetric point  $p^2 = k^2$ . It tends toward a finite value in the infrared and shows an infrared plateau, see e.g. [64].

Within our approach, the dependence on spatial gauge fields and ghosts originates solely from  $A_0 - \bar{A}$  and  $A_0$ -ghost vertices. Such vertices entail that all quantities involved are fully dressed, which is accounted for by using the running coupling,  $g = \bar{g}_k$ , in (38). Furthermore, the coupling  $\bar{g}_k$  in (38) is the renormalisation group (RG)

invariant background running coupling. The combination  $Z_{\bar{A},k}^{1/2} \bar{A}_0$  is RG-invariant, too, and hence  $\bar{\varphi}$  is RG-invariant. Moreover, we also have  $\partial_t(g_k Z_{\bar{A},k}^{1/2} \bar{A}_0) = 0$ , and hence  $\partial_t \bar{\varphi} = 0$ .

Now we use that all background correlations can be expressed in terms of those of the fluctuations with the help of Nielsen identities. In (38) this is particularly simple for the cutoff-independent combination  $\bar{g}_k Z_{\bar{A},k}$ . We rewrite it as

$$\bar{g}_k Z_{\bar{A},k}^{1/2} = g_k Z_{A,k}^{1/2}, \quad Z_{A,k} = \frac{1}{Z_{a,k} Z_{c,k}^2}, \quad g_k = \frac{\bar{g}}{Z_{a,k}^{1/2} Z_{c,k}}, \quad (39)$$

where  $g_k$  and  $Z_{A,k}$  are defined via fluctuating wave-function renormalisations,  $Z_{a/c,k} = Z_{a/c,k}(p_0 = 0, \vec{p}^2 = k^2)$ . Moreover,  $\bar{g}$  is the background coupling at  $k$  with  $Z_{a,k}^{1/2} Z_{c,k} = 1$ . We emphasise that the splitting (39) is not unique, but rather a convenient definition of  $Z_{A,k}$ , enabled by the cutoff independence of the combination  $\bar{g}_k Z_{\bar{A},k}$ .

For non-vanishing temporal fluctuation,  $a_0 \neq 0$ , the parametrisation (38) generalises to

$$2\pi\varphi = \beta g_k Z_{A,k}^{1/2} \left( \bar{A}_0 + \frac{Z_{a,k}^{1/2}}{Z_{A,k}^{1/2}} a_0 \right). \quad (40)$$

Note that the combination (40) is RG-invariant, but not  $t$ -independent for  $a_0 \neq 0$ . Moreover, it is the choice of the splitting (39) and the relation of  $Z_{A,k}$  to the fluctuation wave-function renormalisations that leads to the simple ratio  $Z_{a,k}^{1/2}/Z_{A,k}^{1/2}$  in (40): taking derivatives w.r.t. the fluctuation fields naturally leads to powers of the wave-function renormalisation and the fluctuation coupling  $g_k Z_a^{1/2}$ , see the vertex parametrisation [65] It has been shown in [6] that this approximation of the vertices is quantitatively reliable. The ratio is then given by

$$\frac{Z_{a,k}^{1/2}}{Z_{A,k}^{1/2}} = \frac{1}{Z_{c,k}}. \quad (41)$$

With these prerequisites we can now apply the flow (32) to  $\langle L[A_0] \rangle$ . To this end we employ the parametrisation

$$\langle L[A_0] \rangle = Z_{L,k}[\bar{A}, \phi] \cdot L(\varphi), \quad (42)$$

where the relative factor,  $Z_{L,k}[\bar{A}, \phi]$ , depends on all fluctuation fields  $\phi$  and on the background field  $\bar{A}$ . Furthermore we have  $\phi = \phi(\varphi)$  via (40). It is the renormalisation factor of the composite operator  $L$ , in analogy to the wave-function renormalisation  $Z_\phi$  of the field operators  $\phi$ .

The  $t$ -derivative on the left-hand side of (32) is taken at fixed background  $\bar{A}_0$ . As we have seen above, this corresponds to  $\partial_t \bar{\varphi} = 0$ , which implies  $\partial_t L(\bar{\varphi}) = 0$  and



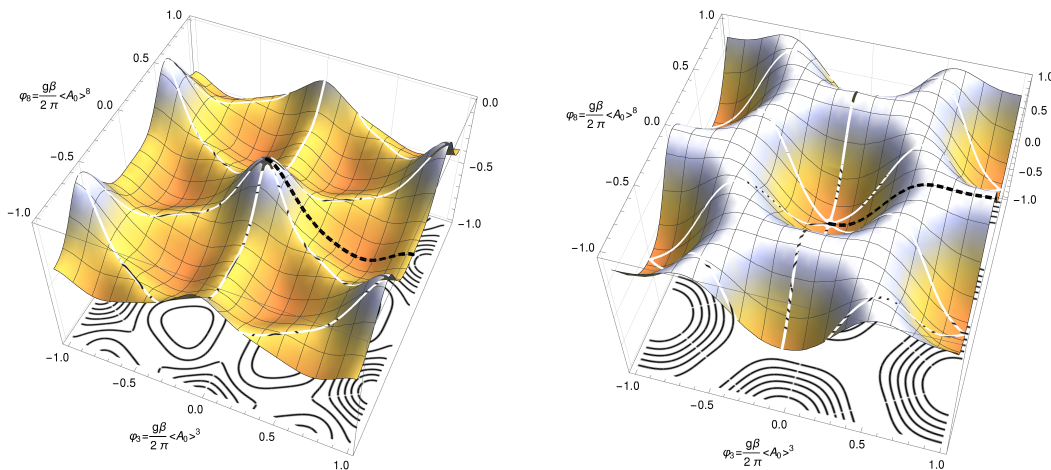


FIG. 4. The infrared glue potential,  $V(\varphi_3, \varphi_8)$ , is shown in the confined phase (left,  $T = 236$  MeV) and in the deconfined phase (right,  $T = 384$  MeV). The periodicity of the potential, discussed in Sec. II is obvious. We restrict ourselves to the line  $\varphi_8 = 0$  and  $\varphi_3 \geq 0$  (indicated by the black, dashed line), where one of the equivalent minima is always found, and where  $L[\langle A_0 \rangle]$  is real and positive semi-definite, cf. Fig. 5.

leads to the flow equation

$$\begin{aligned} \partial_t \langle L \rangle &= L \partial_t Z_{L,k} \\ &= - \frac{g_k^2 Z_{a,k} \beta}{8\pi^2} \int \frac{d^3 p}{(2\pi)^3} \left[ G_k \dot{R}_k G_k \right]_{ab} (\omega_0 = 0, \vec{p}) \\ &\quad \times (Z_{L,k} L^{ba} + Z_{L,k}^b L^a + Z_{L,k}^a L^b + Z_{L,k}^{ba} L), \end{aligned} \quad (43)$$

with gauge group indices  $a, b = 1, \dots, N^2 - 1$  in  $SU(N)$ . For the sake of brevity we have dropped the  $\varphi$ -arguments on the right-hand side and have introduced the notation

$$X^a = \frac{\partial X}{\partial \varphi_a}, \quad X^{ab} = \frac{\partial^2 X}{\partial \varphi_a \partial \varphi_b}, \quad (44)$$

with  $X = L, Z_L$ . The  $x_0$ -independence of  $\langle A_0 \rangle$ , due to the Polyakov gauge for the background field, entails that only the lowest Matsubara frequency,  $\omega_0 = 0$ , is present in this equation. Furthermore, in this gauge only the derivatives with  $a, b = 3, 8$  are non-vanishing in (43). Upon taking the trace, only the components of the propagators that carry no explicit dependence on the background field remain. Hence, the only field dependence on the right-hand side is that of  $L(\varphi)$  and  $Z_{L,k}$ . As the field-dependence of the latter is only generated by the flow, we conclude that the whole field dependence originates from  $L(\varphi)$ . Note also that the above analysis also holds for general constant backgrounds without gauge fixing. In summary, the symmetry properties of  $L(\varphi)$  under shifts and center transformations are carried over to  $\langle L[A_0] \rangle$  via the flow (43).

Eq. (43) effectively is a flow equation for the ratio  $Z_{L,k}$  of the two order parameters,  $L(\varphi) = L[\langle A_0 \rangle(\varphi)]$  and  $\langle L \rangle(\varphi)$  for general background  $\varphi$ . Eventually we evaluate all observables at the minimum  $\bar{\varphi}$  defined by (25).  $Z_{L,k}$  provides a measure for the different impact

of quantum and thermal fluctuation on the two definitions of the Polyakov loop. It hence is a measure of the non-Gaussianity of Polyakov loop correlations as well as of gauge field correlations that is relevant for low energy effective models. The seeming parametric singularity of (43) when  $L(\varphi) = 0$  is lifted by our parametrisation (42), which guarantees that in this case also  $\langle L \rangle = 0$ , cf. Eq. (27).

It is also worth noting that the off-diagonal entries in the last line of Eq. (43) in general are non-vanishing and purely imaginary. They couple to the off-diagonal terms of the propagator,  $G_k^{38}, G_k^{83}$ , which are only present at finite quark chemical potential. This property facilitates the emergence of different, real values for the Polyakov loop and its conjugate,  $\langle L \rangle$  and  $\langle L^\dagger \rangle$ , at finite density. This is expected since these observables relate to the free energies of quarks and anti-quarks, respectively.

Additionally, knowledge of  $Z_{L,k}$  enables us to translate between the glue effective potential,  $V(\varphi)$ , cf. Eq. (24), as computed in [2, 9–13, 16–18, 20–22], and the Polyakov loop potential used in models,  $V_L(L = \langle L \rangle)$  by the above relation  $\langle L \rangle(\varphi) = Z_L(\varphi) L[\varphi]$ . This can, for example, be used to evaluate and improve model potentials.

### C. Input

In order to solve the flow (43), the scale-dependent YM propagators and the glue potential,  $V_k(\varphi)$ , are the only inputs needed. The covariant tensor  $f(D, A_0)$  is directly related to the background potential via (40), to wit

$$f(D, A_0) = Z_{a,k} \beta^2 \frac{g_k^2}{4\pi^2} V_k^{ab}(\varphi). \quad (45)$$

Here the prefactor  $Z_{a,k}$  carries the correct RG-scaling of a gluonic two-point correlation function of the fluctuation



field, and the rest is RG-invariant. FRG calculations for the YM propagators have previously been put forward in [54], and an FRG approach to the glue potential has been presented in, e.g., [12]. Here we build upon these results to achieve a consistent description of fluctuation effects on the Polyakov loop.

First, we briefly recapitulate the calculation of the glue potential, whose flow equation is depicted diagrammatically in Fig. 2. To solve this equation we make use of the temperature- and scale-dependent results for the ghost and gluon propagators from [54]. There, results have been obtained with the ghost and gluon regulators

$$R_{a/c,k}(p^2) = \bar{Z}_{a/c,k} p^2 r(p^2/k^2), \quad r(x) = \frac{x}{e^{x^2} - 1}, \quad (46)$$

which ensures the necessary momentum locality of the flow, as well as an exponential thermal decay proportional to  $k/T$  for large cutoff scales. The wave-function renormalisations  $\bar{Z}_{a/c}$  are related to  $Z_{a/c}$ , for details see [54]. It has been shown in [12] that the corresponding glue potential correctly reproduces the order and critical temperature of the  $SU(3)$  deconfinement phase transition. The resulting glue potential,  $V_{k \rightarrow 0}(\varphi_3, \varphi_8)$ , is shown in Fig. 4 in the confined (left) and deconfined phase (right). The symmetries discussed in Sec. II are clearly visible and we have indicated the line  $\varphi_8 = 0, \varphi_3 \geq 0$ , to which we restrict, by the black, dashed line. The corresponding potential along this line is then shown in Fig. 5 for several temperatures below and above the critical temperature,  $T_c = 264 \pm 26$  MeV. As also discussed in [12], the absolute scale in this computation is set by a comparison of the peak position in the propagators with the lattice [66–68], which results in an error in  $T_c$  of about 10 %.

The physical gauge field,  $\langle A_0 \rangle \sim \bar{\varphi}$ , is determined as the global minimum of the infrared glue potential,  $V_{k \rightarrow 0}$ , see (25). The order parameter  $L(\bar{\varphi})$  is calculated via Eq. (13). FRG data for the YM propagators are available up to  $T \lesssim 1.1$  GeV [12], which allows us to compute the glue potential fully non-perturbatively up to this scale. For all temperatures the glue potential  $V(\varphi)$  can be fitted well via the perturbative Weiss potential as

$$V(\varphi) = a(T) V_W^{\text{SU}(3)}(\varphi) + b(T) V_W^{\text{SU}(3)}(\varphi)^2, \quad (47)$$

where the Weiss potential for  $SU(2)$  is given by  $V_W^{\text{SU}(2)}(\varphi) = (1 - (1 - 2\varphi)^2)^2$  and its  $SU(3)$ -counterpart can be constructed in the standard way as

$$V_W^{\text{SU}(N)}(\varphi) = \frac{1}{2} \sum_{n=1}^{N^2-1} V_W^{\text{SU}(2)}(x_n(\varphi)), \quad (48)$$

with  $x_n = \{0, \pm\varphi_3, \pm\frac{\varphi_3 \pm \sqrt{3}\varphi_8}{2}\}$  in  $SU(3)$  see e.g. [11]. For high temperatures,  $T \gtrsim 1$  GeV we find that the coefficient  $b(T)$  is rather small and the potential is well approximated by the perturbative form. We exploit this observation in the following and replace the glue potential in (45) by the Weiss potential at  $T \gtrsim 1$  GeV.

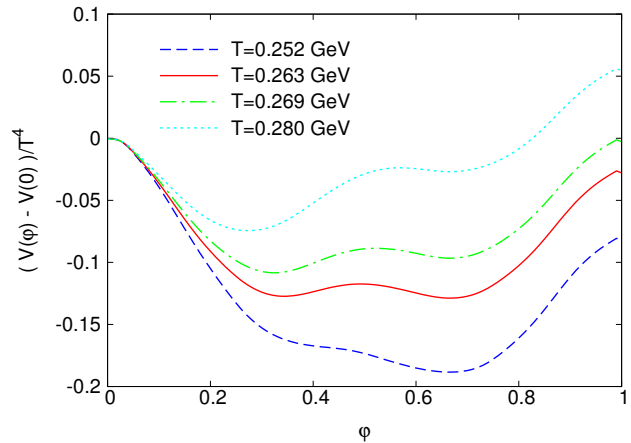


FIG. 5. FRG result for the  $SU(3)$  glue potential along the line  $\varphi_3 \geq 0, \varphi_8 = 0$  for various temperatures. The critical temperature, associated with the first-order transition is given by  $T_c = 264 \pm 26$  MeV.

Furthermore, it turns out that the thermal propagators can be approximated by the  $T = 0$  propagators plus a Debye mass which is fitted to the data. At large temperatures,  $T \gtrsim 1$  GeV, where no FRG data for the propagators is available yet, we use this construction. We have checked that the detailed form of the mass term has little impact on the resulting Polyakov loop. In the plots shown in the next section, we indicate the scale where we switch from first-principles data to the fit for the Debye mass and Weiss potential by a dashed, vertical line.

To finally solve the flow (43) for  $\langle L[A_0] \rangle$ , the last remaining ingredient is the running coupling,  $g_k$ . Within our approach, it is related to the strength of the ghost-gluon vertex,  $g_k^2 \sim Z_{a,k}^{-1} Z_{c,k}^{-2}$ , and can also be deduced from the propagators, cf. [54].

## V. FLUCTUATIONS AND RENORMALISATION

Following the procedure outlined in the last section we are now in the position to compute both Polyakov loops,  $L(\bar{\varphi})$  and  $\langle L \rangle = Z_{L,k=0}(\bar{\varphi}) L(\bar{\varphi})$ . For the computation of the latter we first remark that the composite operator  $\langle L \rangle$  is UV-relevant and has to be renormalised. In the present functional renormalisation group approach the renormalisation procedure is easily accessible. It simply entails that

$$\Lambda \partial_\Lambda \langle L \rangle_{k=0} \stackrel{!}{=} 0, \quad (49)$$

for the renormalised traced Polyakov loop: the expectation value  $\langle L[A_0] \rangle$  at vanishing cutoff scale,  $k = 0$ , does not depend on the initial cutoff scale,  $k = \Lambda$ . Hence, this amounts to adjusting the  $\Lambda$ -dependence of  $\langle L[A_0] \rangle_\Lambda$ . For (49) to hold,  $\langle L[A_0] \rangle_\Lambda$  has to satisfy the flow equation (43), see e.g. [55]. Within the parametrisation (42) this

translates into the requirement that  $Z_{L,\Lambda}$  has to satisfy (43). In turn, the unrenormalised traced Polyakov loop is defined by using the trivial initial condition  $Z_{L,\Lambda} = 1$ , which violates (49). Thus, the multiplicative factor  $Z_{L,\Lambda}$  carries the renormalisation of the Polyakov loop  $\langle L[A_0] \rangle$ , and is related to the multiplicative renormalisation factor  $Z_{\text{lat}}$  used on the lattice.

For asymptotically large scales, that is  $\Lambda/\Lambda_{\text{QCD}} \rightarrow \infty$  and  $\Lambda/T_{\text{max}} \rightarrow \infty$ , it is sufficient to solve (49) up to sub-leading terms that vanish in this limit. Asymptotically large  $\Lambda/\Lambda_{\text{QCD}}$  guarantees the perturbative limit that facilitates the computation of the initial  $Z_L$ . The second requirement,  $\Lambda/T_{\text{max}} \rightarrow \infty$  guarantees the temperature-independence of the initial condition.

In the above asymptotic limit, the temperature dependence of the gluon propagators, including the term proportional to the potential curvature  $V^{ab}$ , and of the gluonic wave-function renormalisation  $Z_a$  decays exponentially with  $\exp\{-c(r)k/T\}$ , see [12, 54, 69]. The prefactor  $c(r)$  depends on the shape function  $r$  in (46), and vanishes for non-analytic regulators, see [69]. In such a case the thermal suppression is only polynomial in  $T/k$ . For the present regulators, (46), we have an exponential decay. The same exponential decay holds for general correlation functions, and hence also applies to the coupling  $\alpha_s$ . Accordingly, the temperature dependence of the flow (43) decays exponentially, reflecting the temperature independence of the UV renormalisation. Moreover, the flow also becomes  $\varphi$ -independent exponentially fast as the sum of the  $L^{ab}$ -terms is proportional to  $L$  for vacuum propagators which are proportional to  $\delta^{ab}$ . Hence, all  $Z_L^a, Z_L^{ab}$  terms on the right-hand side can be dropped, and we are left with the asymptotic flow

$$\frac{\partial_t Z_{L,k}}{Z_{L,k}} = \frac{g_k^2 Z_{a,k} \beta}{6} \int \frac{d^3 p}{(2\pi)^3} \left[ G_k \dot{R}_k G_k \right]_{bb} (0, \vec{p}), \quad (50)$$

for the renormalisation factor. The prefactor has a logarithmic scaling with  $k$  from both, the running coupling  $g_k^2$  and the gluon wave-function renormalisation  $Z_{a,k}$ . The scaling of the latter is cancelled by the logarithmic scaling of the propagators and regulator. The remaining spatial momentum integral scales linearly with the cutoff scale. Hence we arrive at the total scaling

$$\frac{\partial_t Z_{L,k}}{Z_{L,k}} = z_L \alpha_{s,k} \frac{k}{T}, \quad (51)$$

with the strong running coupling  $\alpha_{s,k} = g_k^2/(4\pi)$  at  $T = 0$  up to exponentially suppressed terms. The factor  $z_L$  is given by

$$z_L = \frac{2\pi}{3} \int \frac{d^3 p}{(2\pi)^3} \frac{1}{k} \left[ Z_{a,k} G_k \dot{R}_k G_k \right]_{bb} (0, \vec{p}), \quad (52)$$

with the propagators  $G_k$  and  $Z_{a,k}$  at vanishing temperature, up to exponentially suppressed terms. Moreover,  $z_L$  tends towards a constant for large cutoff scales,  $z_{L,k \rightarrow \infty} = 0.0177$ .

Note also that the exponential thermal decay does not hold in momentum space at vanishing cutoff scale. All correlation functions, including the propagator and the running coupling,  $\alpha_s(p, T)$ , only show a polynomial decay of the thermal contributions with large momenta, that is with powers of  $T/p$ , similarly to the polynomial decay with  $T/k$  for non-analytic cutoffs. However, contrary to the latter, the polynomial decay with  $T/p$  relates to physics, for example that of the propagator relates to the Tan relations in many-body physics, for a discussion in Yang-Mills theory see [54]. In turn this entails that the choice of temperature-independent renormalisation conditions in a non-perturbative approach based on the running coupling at asymptotic momentum scales is intricate. Hence, in particular the identification of the finite temperature running coupling at large momenta with the  $T = 0$  one,  $\alpha_s(p \gg T, T) = \alpha_s(p \gg T, 0)$  introduces a temperature-dependent renormalisation scheme due to the sub-leading powers of  $T/p$ .

We emphasise that for the present renormalisation scheme with the regulator (46) this is avoided: at large cutoff scales  $k/T \gg 1$  the difference of the couplings  $\alpha_{s,k}(p, T)$  and  $\alpha_{s,k}(p, T = 0)$  is exponentially suppressed with  $f(T/k, T/p) \exp\{-c_T k/T\}$ . Here,  $f(x, y)$  has power law suppressions for both,  $k/T \rightarrow \infty$  and  $p/T \rightarrow \infty$ . At  $k = 0$  the exponential suppression disappears. Hence the integrated flow leads to the sub-leading momentum-dependent terms in the coupling in  $T/p$  that are only power law suppressed at large momentum scales. This has been shown in [54].

Nonetheless, a temperature-dependent renormalisation scheme is a consistent choice, and such a general setting is taken into account in the present setting by allowing for thermal shifts in the cutoff scale. This amounts to a sub-leading change of the initial condition for the flow of  $Z_L$  proportional to  $T/\Lambda$ , and hence a sub-leading contribution to the flow proportional to  $T/\Lambda$ . The flow is peaked at about the temperatures scale, and we are led to the final expression for the renormalisation factor  $Z_{L,\Lambda}$  at asymptotically large cutoff scales  $\Lambda$

$$Z_{L,\Lambda}(T) = e^{a_{\text{cont}} \Lambda/T}, \quad a_{\text{cont}} = a_0 + a_1 \frac{T}{\Lambda} \alpha_s(c_T T) + \dots, \quad (53)$$

where the leading term  $a_0 = 1/\Lambda \int^\Lambda dk z_L \alpha_{s,k}$  is proportional to  $\alpha_{s,\Lambda}$  for large cutoff scales. However, it is very slowly varying due to its only logarithmic decay, and for the chosen initial cutoffs  $\Lambda = 10, 15, 18$  GeV in Fig. 6 it is given by  $a_0 = 0.0175$ . More importantly, Fig. 6 demonstrates the renormalisation group invariance of the traced Polyakov loop observable  $\langle L \rangle$ . The higher-order term, with free coefficient  $a_1$ , acts as a constant shift in the Polyakov loop at low temperatures, and decreases at large  $T$ , respecting the correct high-temperature limit. It implements the subleading temperature-dependent renormalisation discussed above, and the parameters  $a_1, c_T$  specify the scheme. Note also that for small temperatures above, but close to the phase transition the flow for  $Z_L$  is peaked at the mass

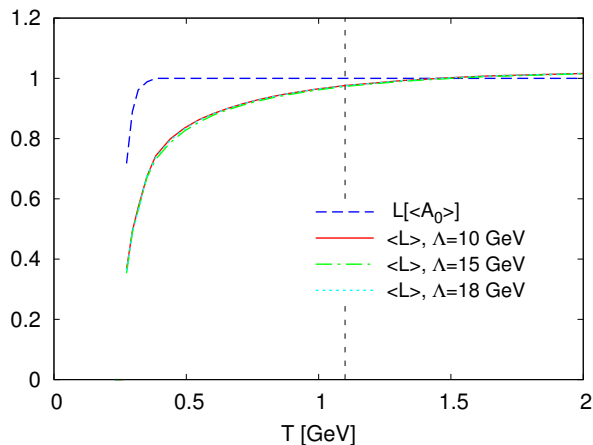


FIG. 6. Demonstration of the cutoff-independence of the Polyakov loop,  $\langle L \rangle$  with  $a_1 = 0$  in (53), and the comparison to  $L[\langle A_0 \rangle]$ . The high-T limit in both cases is unity.

gap of the gluons and the scale  $c_T T$  in  $\alpha_s(c_T T)$  has to freeze at about the mass gap. This entails that the sub-leading term related to the potential temperature-dependent renormalisation provides a constant off-set in the infrared, and the ratio for expectation values of the traced Polyakov loop is independent of the temperature-dependent part of the renormalisation. In summary, the potential temperature-dependent RG scheme introduces in  $Z_L$  a temperature-dependent, but cutoff-independent factor for asymptotically large temperatures, while it is constant for low temperatures due to the plateau in the background coupling. In Fig. 6 we have used  $a_1 = 0$ , since it does not explicitly depend on  $\Lambda$ . This subtlety is discussed further in the next section.

The above renormalisation procedure in the continuum is to be compared to the lattice renormalisation. There, it is known that taking the infinite volume limit at a fixed temperature leads to a vanishing Polyakov loop and an appropriate renormalisation procedure is needed [29–32]. It was suggested already by Polyakov [70], that the linear divergences appearing in  $\langle L \rangle$  at any order in perturbation theory can be combined into an exponential factor. This leads to the definition of the renormalised Polyakov loop

$$\langle L \rangle_{\text{lat}} = Z_{\text{lat}}(T) \langle L \rangle_{\text{bare}}, \quad \text{with} \quad Z_{\text{lat}}(T) = e^{a_{\text{lat}} \Lambda / T}, \quad (54)$$

where (53) suggests  $a_{\text{cont}} = a_{\text{lat}}$  up to differences in the renormalisation condition. On the lattice, the constant  $a_{\text{lat}}$  can be fixed via the zero-temperature heavy-quark potential [29–31], for other renormalisation schemes see e.g. [26, 32–34]. Such a renormalisation procedure is unique only up to a constant, i.e. an overall multiplicative renormalisation remains, cf. [31, 32]. The different normalisations used on the lattice and in the continuum may also introduce a temperature-dependent part of the renormalisation as discussed above. This has to be taken into account in a comparison of the different schemes, which is deferred to the next section.

While both continuum observables,  $L[\langle A_0 \rangle]$  and  $\langle L \rangle$ , serve as order parameters for the confinement-deconfinement transition, Fig. 6 reveals clear differences between the two above  $T_c$ . It had been found previously, and is also confirmed by our data, that the overall shape of  $L[\langle A_0 \rangle]$  is much steeper than that of  $\langle L \rangle$ . The difference between these two observables is quantified by  $Z_{L,k \rightarrow 0}(T)$  and is due to the different impact of thermal and quantum fluctuations on both observables.

First we note that  $L[\langle A_0 \rangle]$  saturates at its high-temperature limit,  $L[\langle A_0 \rangle] \xrightarrow{T \rightarrow \infty} 1$ , already at  $T \gtrsim 0.4$  GeV. In turn,  $\langle L \rangle$  rises much more gradually. It eventually overshoots unity at  $T \approx 1.5$  GeV and approaches its high-T limit of one from above, in agreement with the expectation from perturbation theory [71].

The non-Gaussianity of the Polyakov loop in terms of correlations of the gauge field is quantified by the difference between  $L[\langle A_0 \rangle]$  and  $\langle L \rangle$  as discussed in Sec. III. It is clearly visible in Fig. 6, and originates in two qualitatively different mechanisms: The first one simply encodes the renormalisation of the gauge field correlation functions that are in line with (resummed) thermal perturbation theory. These deviations are similar to those observed in the pressure, which are known to be significant even for temperatures  $T \gg T_c$  as the approach to the Stefan-Boltzmann limit is rather slow. Still, they are captured well by HTL or similar resummation schemes such as (perturbative) two-particle-irreducible computations. This is visible in  $Z_{L,k}$  which is approximately linear in the cutoff scale up to the thermal gap for temperatures  $T \gtrsim (2-3)T_c$ . In turn, for temperatures  $T \lesssim (2-3)T_c$  the factor  $Z_{L,k}$  shows an additional significant drop at about the non-perturbative mass gap of Yang-Mills and freezes below this scale.

In summary, the non-perturbative renormalisation factor  $Z_L(T)$  carries much of the information about the perturbative and non-perturbative thermal and quantum fluctuations. The deviations are particularly large for the low temperature regime  $T \leq (2-3)T_c$ . In this regime we also see a significant non-trivial dynamics related to the confinement-deconfinement phase transition. It is expected that these differences have a significant impact on model calculations if the standard Gaussian approximation is lifted.

## VI. CONTINUUM AND LATTICE RESULTS FOR $\langle L[A_0] \rangle$ AND RENORMALISATION

Now we turn to a comparison of  $\langle L \rangle$  in the continuum and on the lattice. This is done as a function of the reduced temperature,  $T/T_c$ , to accommodate for the differences in the relative scale setting procedure mentioned before. Using the renormalisation procedure discussed above with only  $a_0$ , the ratio of the continuum and lattice Polyakov loop expectation values is given by  $\langle L \rangle_{\text{cont}} / \langle L \rangle_{\text{lat}} = 0.92$  for temperatures  $T/T_c \lesssim 10$ , that is up to about 3 GeV. It has been discussed at length

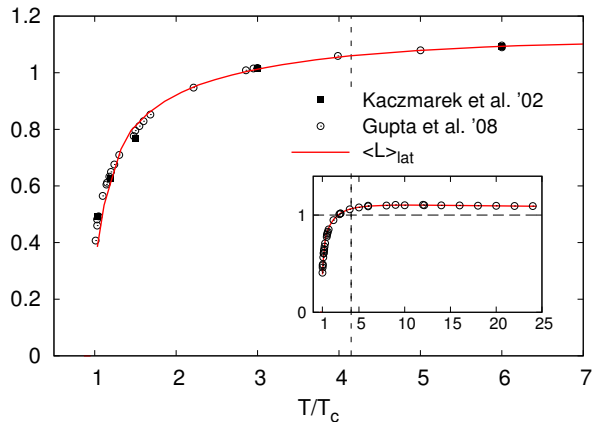


FIG. 7. Polyakov loop,  $\langle L \rangle$ , compared to the renormalised lattice result, [29, 32]. The inset shows the high-T behaviour vs  $T/T_c$ .

in the last section that such a constant low temperature off-set is introduced by a relative temperature-dependent renormalisation. Hence, this result confirms the quantitative agreement of both computations. Above this temperature we observe a change of this ratio towards unity triggered by the normalisation of both Polyakov loops at infinite temperature. As discussed in Sec. V, the subleading term in the continuum renormalisation, that signals a temperature-dependent renormalisation scheme, on the other hand, is approximately constant at low  $T \lesssim 10T_c$ . With the choice  $a_1 = 0.47$  it accounts for the factor  $1.088 = 1/0.92$ , see Fig. 7. Note that this term also accommodates possible sub-leading corrections of the continuum computation in the presence of full gluon propagators for asymptotically large temperatures. In the present work we have tested a large, but not complete set of sub-leading temperature corrections to the propagators, and did not observe any impact. In summary this strongly suggests a relative temperature-dependent renormalisation. To highlight the quantitative agreement up to asymptotically high temperatures, the inset in Fig. 7 shows the continuum Polyakov loop with full renormalisation (54), and the lattice Polyakov loop from [32] vs.  $T/T_c$ . A full investigation of this large temperature intricacy for  $T/T_c \gg 1$  will be discussed elsewhere.

## VII. CONCLUSION AND OUTLOOK

In this work we have discussed different order parameters for the confinement-deconfinement transition in Yang-Mills theory, based on the Polyakov loop variable  $P(\vec{x}) = \exp(2\pi i\varphi)$ . The common order parameter is the expectation value of the traced Polyakov loop,  $\langle L[A_0] \rangle$ , that is related to the free energy of a quark-anti-quark pair. It has been computed on the lattice for both, Yang-Mills theory and full QCD at finite temperature, but

quantitative continuum computations had been missing so far. A further order parameter is related to the expectation value  $\bar{\varphi}$  of the algebra-valued field  $\varphi$ , built from the expectation value of the gauge invariant eigenvalues, see the discussion around (10). With  $\bar{\varphi}$  we can also compute the traced Polyakov loop  $L(\bar{\varphi})$ , an order parameter that bears similarities to  $\langle L[A_0] \rangle$ . The field  $\varphi$  is directly related to the gauge field and its expectation values are  $\langle A_0 \rangle$ . It has first been computed non-perturbatively within continuum approaches to Yang-Mills theory and QCD in [2, 9–12], first lattice results have been presented e.g. in [38, 40]. It has also been argued that Polyakov-loop enhanced low-energy effective models should rather be based on the latter observables,  $\bar{\varphi}$  and  $L(\bar{\varphi})$ , than on the former,  $\langle L[A_0] \rangle$ , see e.g. [2–5, 8, 52].

We have argued that the order parameters  $\langle L[A_0] \rangle$  and  $L(\bar{\varphi})$  agree within Gaussian approximations for correlations of the temporal gauge field  $A_0$  or  $\varphi$ , and consequently within such an approximation for the correlations of  $L$ , see the discussion around Eqs. (26) to (29) on page 5. Low-energy effective models built on  $\langle L[A_0] \rangle$  rest on these Gaussian approximations for the computation of the quark-gauge field or rather quark-Polyakov loop fluctuations. In contradistinction, models built on  $\bar{\varphi}$  are not subject to these Gaussian approximations as they can be derived directly from QCD. The difference between  $\langle L[A_0] \rangle$  and  $L(\bar{\varphi})$  is a direct measure for the non-Gaussianity of these fluctuations, and hence a measure for the quantitative reliability of  $\langle L[A_0] \rangle$ -based models.

In the present work we have discussed the differences and similarities of these observables. We have also provided a review of the underlying symmetries and in particular of the connection of the algebra-valued field  $\varphi$  to the gauge field, which is the basis of continuum formulations of Yang-Mills theories. The background glue potential in Yang-Mills theory has been computed within the functional renormalisation group, similarly to [9, 11, 12]. Using the flow equation for general composite operators put forward in [55] we have furthermore derived a flow equation for  $\langle L[A_0] \rangle$ . This flow equation is fully non-perturbative and also utilises the expectation value  $\bar{\varphi}$ . The difficult task of computing infinite-order correlation functions of the gauge field is resolved within the successive integration of momentum fluctuations: each iterative infinitesimal momentum-shell integration increases the order of gauge field fluctuations taken into account.

We have shown in Sec. V that the present continuum computation of  $\langle L[A_0] \rangle$  is renormalisation group invariant. Moreover, the present functional renormalisation group approach provides a direct and simple access to the renormalisation procedure. This also allows us to discuss the relative renormalisation between the lattice and present continuum computations for  $\langle L[A_0] \rangle$ . It has been argued that it amounts to a temperature-dependent renormalisation at large temperatures, see Sec. V.

In Sec. VI we have shown that the results for  $\langle L[A_0] \rangle$  within the present non-perturbative continuum approach agree quantitatively with the lattice results, see Fig. 7.

As the present continuum computation of  $\langle L[A_0] \rangle$  is based on the input  $\bar{\varphi}$  or rather  $\langle A_0 \rangle$ , it also is a further non-trivial support for the quantitative reliability of the results for  $\langle A_0 \rangle$  in [2, 9–12], and related applications in QCD-enhanced low energy effective models [4, 5, 52].

We have shown that the non-Gaussianity of the fluctuations grows strong in the regime  $T \lesssim 3T_c$  which is the regime of interest for the low energy effective models, see Fig. 6. This suggests that, in particular for an analysis of fluctuations in QCD, it is important to take into account the Polyakov loop fluctuations if one aims at quantitative precision. This can either be done by using models based on  $\bar{\varphi}$  or  $\langle A_0 \rangle$ , or by amending the  $\langle L[A_0] \rangle$ -based effective models by a fluctuation analysis of the Polyakov loop.

In turn, both order parameters are well described by (resummed) perturbation theory for temperatures  $T \gtrsim 3T_c$ . Such a behaviour is already well-known from the trace anomaly. In the present continuum approach in the Landau-deWitt gauge it can be traced back to the non-perturbative mass-gap in the gluon propagator. Even though the propagator is a gauge-dependent quantity, this mass-gap reflects the mass-gap in Yang-Mills theory, and is directly related to confinement.

Finally, the extension of the presented approach to other gauge groups, such as  $SU(2)$  or  $SU(N)$  with  $N > 3$  and exceptional Lie groups, as well full QCD is straightforward and relies solely on the knowledge of the corresponding propagators. Here, the case of QCD with  $N_f$  quark flavours is of particular interest: the corresponding unquenched propagators and unquenching of the glue potential have been put forward in [2, 13]. The structure of the flow equation (43) then suggests that a splitting between  $\langle L \rangle$  and  $\langle L^\dagger \rangle$  will arise naturally, accounting for the fact that these objects are related to the free energies of quarks and anti-quarks, respectively. Furthermore, since light quarks break the center symmetry explicitly, the confinement-deconfinement

transition is a crossover in this case. The temperature-dependent differences between  $L[\langle A_0 \rangle]$  and  $\langle L \rangle$ , as observed here, then have a drastic impact on the pseudo-critical temperature, usually deduced from the inflection point of these observables. Indeed, the order parameter  $L(\langle A_0 \rangle)$  has been computed with continuum methods in  $N_f = 2$  flavour QCD in [2] for finite temperature and imaginary chemical potential, and in  $N_f = 2 + 1$  flavour QCD in [13] for finite temperature and real chemical potential. As expected, both show a significantly steeper thermal rise in comparison to the lattice results for  $\langle L \rangle$ , see e.g. [72] for  $N_f = 2 + 1$  flavour results. Moreover, the pseudo-critical temperature of  $L[\langle A_0 \rangle]$  for the confinement-deconfinement phase transition agrees well with the chiral pseudo-critical temperature, see [2, 13]. From the present work it is clear that this originates in the different treatment of non-Gaussian fluctuations in the order parameters. The close chiral and confinement-deconfinement transition temperatures also suggests that the observable  $L[\langle A_0 \rangle]$  shows a closer resemblance to baryonic fluctuation observables that have a direct physics interpretation in dynamical QCD.

In summary, this work lays the foundation for a systematic study of the confinement-deconfinement transition in the phase diagram of QCD, both in model approaches and from first principles.

### Acknowledgements

We thank the fQCD collaboration, in particular L. Fister, for discussions and collaboration on related topics. This work is supported by the Helmholtz Alliance HA216/EMMI, by ERC-AdG-290623 and by the BMBF grant OSPL2VHCTG.

- 
- [1] W.-j. Fu and J. M. Pawłowski, (2015), arXiv:1508.06504 [hep-ph].
  - [2] J. Braun, L. M. Haas, F. Marhauser, and J. M. Pawłowski, Phys.Rev.Lett. **106**, 022002 (2011), arXiv:0908.0008 [hep-ph].
  - [3] J. M. Pawłowski, AIP Conf.Proc. **1343**, 75 (2011), arXiv:1012.5075 [hep-ph].
  - [4] L. M. Haas, R. Stiele, J. Braun, J. M. Pawłowski, and J. Schaffner-Bielich, Phys.Rev. **D87**, 076004 (2013), arXiv:1302.1993 [hep-ph].
  - [5] T. K. Herbst, M. Mitter, J. M. Pawłowski, B.-J. Schaefer, and R. Stiele, Phys.Lett. **B731**, 248 (2014), arXiv:1308.3621 [hep-ph].
  - [6] M. Mitter, J. M. Pawłowski, and N. Strodthoff, Phys. Rev. **D91**, 054035 (2015), arXiv:1411.7978 [hep-ph].
  - [7] J. Braun, L. Fister, J. M. Pawłowski, and F. Rennecke, (2014), arXiv:1412.1045 [hep-ph].
  - [8] J. M. Pawłowski, Nucl. Phys. **A931**, 113 (2014).
  - [9] J. Braun, H. Gies, and J. M. Pawłowski, Phys.Lett. **B684**, 262 (2010), arXiv:0708.2413 [hep-th].
  - [10] F. Marhauser and J. M. Pawłowski, (2008), arXiv:0812.1144 [hep-ph].
  - [11] J. Braun, A. Eichhorn, H. Gies, and J. M. Pawłowski, Eur.Phys.J. **C70**, 689 (2010), arXiv:1007.2619 [hep-ph].
  - [12] L. Fister and J. M. Pawłowski, Phys.Rev. **D88**, 045010 (2013), arXiv:1301.4163 [hep-ph].
  - [13] C. S. Fischer, L. Fister, J. Luecker, and J. M. Pawłowski, Phys.Lett. **B732**, 273 (2014), arXiv:1306.6022 [hep-ph].
  - [14] C. S. Fischer, J. Luecker, and J. M. Pawłowski, Phys. Rev. **D91**, 014024 (2015), arXiv:1409.8462 [hep-ph].
  - [15] C. S. Fischer, J. Luecker, and C. A. Welzbacher, Phys. Rev. **D90**, 034022 (2014), arXiv:1405.4762 [hep-ph].
  - [16] H. Reinhardt and J. Heffner, Phys.Lett. **B718**, 672 (2012), arXiv:1210.1742 [hep-th].
  - [17] H. Reinhardt and J. Heffner, Phys.Rev. **D88**, 045024 (2013), arXiv:1304.2980 [hep-th].

- [18] J. Heffner and H. Reinhardt, Phys. Rev. **D91**, 085022 (2015), arXiv:1501.05858 [hep-th].
- [19] K.-I. Kondo, Phys. Rev. **D82**, 065024 (2010), arXiv:1005.0314 [hep-th].
- [20] K. Fukushima and K. Kashiwa, Phys.Lett. **B723**, 360 (2013), arXiv:1206.0685 [hep-ph].
- [21] U. Reinosa, J. Serreau, M. Tissier, and N. Wschebor, Phys.Lett. **B742**, 61 (2015), arXiv:1407.6469 [hep-ph].
- [22] U. Reinosa, J. Serreau, M. Tissier, and N. Wschebor, Phys.Rev. **D91**, 045035 (2015), arXiv:1412.5672 [hep-th].
- [23] K.-I. Kondo, (2015), arXiv:1508.02656 [hep-th].
- [24] C. Ford, U. Mitreuter, T. Tok, A. Wipf, and J. Pawłowski, Annals Phys. **269**, 26 (1998), arXiv:hep-th/9802191 [hep-th].
- [25] P. van Baal, (2000), arXiv:hep-ph/0008206 [hep-ph].
- [26] A. Mykkanen, M. Panero, and K. Rummukainen, JHEP **05**, 069 (2012), arXiv:1202.2762 [hep-lat].
- [27] P. de Forcrand and O. Jahn, Nucl. Phys. **B651**, 125 (2003), arXiv:hep-lat/0211004 [hep-lat].
- [28] G. Boyd, J. Engels, F. Karsch, E. Laermann, C. Legeland, *et al.*, Nucl.Phys. **B469**, 419 (1996), arXiv:hep-lat/9602007 [hep-lat].
- [29] O. Kaczmarek, F. Karsch, P. Petreczky, and F. Zantow, Phys.Lett. **B543**, 41 (2002), arXiv:hep-lat/0207002 [hep-lat].
- [30] F. Zantow, (2003), arXiv:hep-lat/0301014 [hep-lat].
- [31] S. Gupta, K. Huebner, and O. Kaczmarek, Nucl.Phys. **A785**, 278 (2007), arXiv:hep-lat/0608014 [hep-lat].
- [32] S. Gupta, K. Huebner, and O. Kaczmarek, Phys. Rev. **D77**, 034503 (2008), arXiv:0711.2251 [hep-lat].
- [33] A. Dumitru, Y. Hatta, J. Lenaghan, K. Orginos, and R. D. Pisarski, Phys.Rev. **D70**, 034511 (2004), arXiv:hep-th/0311223 [hep-th].
- [34] R. V. Gavai, Phys. Lett. **B691**, 146 (2010), arXiv:1001.4977 [hep-lat].
- [35] L. Abbott, Nuclear Physics B **185**, 189 (1981).
- [36] D. J. Gross, R. D. Pisarski, and L. G. Yaffe, Rev. Mod. Phys. **53**, 43 (1981).
- [37] N. Weiss, Phys. Rev. **D24**, 475 (1981).
- [38] D. Diakonov, V. Petrov, H.-P. Schadler, and C. Gattringer, JHEP **11**, 207 (2013), arXiv:1308.2328 [hep-lat].
- [39] J. Greensite, Phys.Rev. **D86**, 114507 (2012), arXiv:1209.5697 [hep-lat].
- [40] K. Langfeld and J. M. Pawłowski, Phys. Rev. **D88**, 071502 (2013), arXiv:1307.0455 [hep-lat].
- [41] K. Fukushima, Phys.Lett. **B591**, 277 (2004), arXiv:hep-ph/0310121.
- [42] E. Megias, E. Ruiz Arriola, and L. Salcedo, Phys.Rev. **D74**, 065005 (2006), arXiv:hep-ph/0412308.
- [43] C. Ratti, M. A. Thaler, and W. Weise, Phys.Rev. **D73**, 014019 (2006), arXiv:hep-ph/0506234.
- [44] S. Mukherjee, M. G. Mustafa, and R. Ray, Phys.Rev. **D75**, 094015 (2007), arXiv:hep-ph/0609249 [hep-ph].
- [45] S. Roessner, C. Ratti, and W. Weise, Phys.Rev. **D75**, 034007 (2007), arXiv:hep-ph/0609281.
- [46] B.-J. Schaefer, J. M. Pawłowski, and J. Wambach, Phys.Rev. **D76**, 074023 (2007), arXiv:0704.3234 [hep-ph].
- [47] K. Fukushima, Phys.Rev. **D77**, 114028 (2008), arXiv:0803.3318 [hep-ph].
- [48] T. K. Herbst, J. M. Pawłowski, and B.-J. Schaefer, Phys.Lett. **B696**, 58 (2011), arXiv:1008.0081 [hep-ph].
- [49] V. Skokov, B. Friman, and K. Redlich, Phys.Rev. **C83**, 054904 (2011), arXiv:1008.4570 [hep-ph].
- [50] V. Skokov, B. Stokic, B. Friman, and K. Redlich, Phys. Rev. **C82**, 015206 (2010), arXiv:1004.2665 [hep-ph].
- [51] B.-J. Schaefer and M. Wagner, Phys.Rev. **D85**, 034027 (2012), arXiv:1111.6871 [hep-ph].
- [52] T. K. Herbst, J. M. Pawłowski, and B.-J. Schaefer, Phys. Rev. **D88**, 014007 (2013), arXiv:1302.1426 [hep-ph].
- [53] C. Wetterich, Phys.Lett. **B301**, 90 (1993).
- [54] L. Fister and J. M. Pawłowski, (2011), arXiv:1112.5440 [hep-ph].
- [55] J. M. Pawłowski, Annals Phys. **322**, 2831 (2007), arXiv:hep-th/0512261.
- [56] D. F. Litim and J. M. Pawłowski, World Sci. , 168 (1999), arXiv:hep-th/9901063.
- [57] J. Berges, N. Tetradis, and C. Wetterich, Phys.Rept. **363**, 223 (2002), arXiv:hep-ph/0005122.
- [58] J. Polonyi, Central Eur.J.Phys. **1**, 1 (2003), arXiv:hep-th/0110026 [hep-th].
- [59] H. Gies, Lect.Notes Phys. **852**, 287 (2012), arXiv:hep-ph/0611146.
- [60] B.-J. Schaefer and J. Wambach, Phys.Part.Nucl. **39**, 1025 (2008), arXiv:hep-ph/0611191.
- [61] O. J. Rosten, Phys. Rept. **511**, 177 (2012), arXiv:1003.1366 [hep-th].
- [62] J. Braun, J.Phys. **G39**, 033001 (2012), arXiv:1108.4449 [hep-ph].
- [63] L. von Smekal, Nucl.Phys.Proc.Suppl. **228**, 179 (2012), arXiv:1205.4205 [hep-ph].
- [64] A. Eichhorn, H. Gies, and J. M. Pawłowski, Phys.Rev. **D83**, 045014 (2011), arXiv:1010.2153 [hep-ph].
- [65] C. S. Fischer and J. M. Pawłowski, Phys. Rev. **D80**, 025023 (2009), arXiv:0903.2193 [hep-th].
- [66] A. Maas, Phys.Rept. **524**, 203 (2013), arXiv:1106.3942 [hep-ph].
- [67] C. S. Fischer, A. Maas, and J. A. Müller, Eur. Phys. J. **C68**, 165 (2010), arXiv:1003.1960 [hep-ph].
- [68] A. Maas, J. M. Pawłowski, L. von Smekal, and D. Spielmann, Phys. Rev. **D85**, 034037 (2012), arXiv:1110.6340 [hep-lat].
- [69] L. Fister and J. M. Pawłowski, (2015), arXiv:1504.05166 [hep-ph].
- [70] A. Polyakov, Nuclear Physics B **164**, 171 (1980).
- [71] E. Gava and R. Jengo, Physics Letters B **105**, 285 (1981).
- [72] S. Borsanyi *et al.* (Wuppertal-Budapest Collaboration), JHEP **1009**, 073 (2010), arXiv:1005.3508 [hep-lat].